Check for updates

A$_2$SrM^{IV}S$_4$ (A = Li, Na; M^{IV} = Ge, Sn) concurrently exhibiting wide bandgaps and good nonlinear optical responses as new potential infrared nonlinear optical materials†

Kui Wu, [ID] ‡[a] Yu Chu,‡[bc] Zhihua Yang [ID] [b] and Shilie Pan [ID] *[b]

Exploration of new nonlinear optical (NLO) materials is of importance for infrared (IR) applications. However, it is an extremely tough challenge to design and synthesize excellent IR NLO materials with optimal performances (*e.g.*, concurrently a large NLO response and wide bandgap). Herein, four new mixed alkali/alkaline earth metal sulfides, A$_2$SrM^{IV}S$_4$ (A = Li, Na; M^{IV} = Ge, Sn), were successfully synthesized by a motif-optimization approach using the classical AgGaS$_2$ as a template. Note that all of them concurrently exhibit wide bandgaps (3.1–3.8 eV) and good NLO responses (0.5–0.8 × AgGaS$_2$) with phase-matching behavior, which satisfy the balance conditions (E$_g$ ≥ 3.0 eV and d$_{ij}$ ≥ 0.5 × benchmark AgGaS$_2$) of optical performances and hence are outstanding IR NLO materials. Remarkably, both of Na$_2$SrM^{IV}S$_4$ have the same structure without the structural transformation (Ge to Sn) in the reported related analogues and an interesting cation-dependent structural change is also found in Na$_2$M^{II}SnS$_4$ (M^{II}: Sr, R3c *vs.* Ba, *I*$\bar{4}$2d). These results verify that the above design strategy of motif-optimization provides a feasible guide for the discovery of new IR NLO candidates and the A–AE–M–S (A = alkali metal; AE = alkaline-earth metal; M = Ga, In, Ge, Sn) system was identified as the preferred system for IR NLO materials.

Introduction

Nonlinear optical (NLO) materials are of great importance in achieving the output of tunable lasers ranging from ultraviolet (UV)/deep-UV to the infrared (IR) region.[1] In the deep-UV to visible regions, many kinds of oxides including borates,[2] phosphates,[3] carbonates,[4] and iodates[5] have been developed as worth exploring systems for the discovery of NLO candidates. Unfortunately, most oxides are limited in the IR region because of their low IR absorption edges induced by the strong absorption of metal/metalloid-oxygen bands. So far, commercially available

NLO materials have been rarely discovered in the IR region and all of them still exhibit some inherent performance drawbacks (low laser damage threshold (LDT) and two-photon absorption (TPA)) that seriously hinder their wide applications.[6] Therefore, a critical prerequisite for the future exploration of IR NLO materials is to achieve a suitable balance between the large second harmonic generation (SHG) response (d$_{ij}$) and wide bandgap (E$_g$) in view of their inversely proportional relationship; thus, the two important parameters (E$_g$ and d$_{ij}$) must satisfy the following balance conditions (E$_g$ ≥ 3.0 eV and d$_{ij}$ ≥ 0.5 × benchmark AgGaS$_2$) for one outstanding IR NLO material.[7] After decades of exploration and development, hundreds of IR NLO materials have been synthesized and note that chalcogenides are the main research source for the exploration of new IR NLO materials.[8] The previously reported results show that by incorporation of the second-order Jahn–Teller (SOJT) effect d^0 transition-metals or/and lone-pair cations into crystal structures it is hard to obtain suitable balanced performances for IR NLO materials.[9] Thus, an efficient design strategy that could enhance the E$_g$ and simultaneously maintain good d$_{ij}$ appears to be particularly important. After a detailed literature survey, to the best of our knowledge, about dozens of chalcogenides satisfy the demand of performance balance so far and most of them are sulfides.[10] Besides, this investigation also shows that almost all their cations are alkali or/and alkaline earth metals without d–d or f–f electronic

[a]*College of Chemistry and Environmental Science, Hebei University, Key Laboratory of Analytical Science and Technology of Hebei Province, Baoding 071002, China*

[b]*CAS Key Laboratory of Functional Materials and Devices for Special Environments, Xinjiang Technical Institute of Physics & Chemistry, CAS, Xinjiang Key Laboratory of Electronic Information Materials and Devices, 40-1 South Beijing Road, Urumqi 830011, China. E-mail: slpan@ms.xjb.ac.cn*

[c]*Center of Materials Science and Optoelectronics Engineering, University of Chinese Academy of Sciences, Beijing 100049, China*

† Electronic supplementary information (ESI) available: Experimental details, structural distortion, BVS and GII, performance comparison, LDTs, powder XRD, BS and DOS. CCDC 1888059, 1888058, 1888057, and 1888060 for Li$_2$SrGeS$_4$, Li$_2$SrSnS$_4$, Na$_2$SrGeS$_4$, and Na$_2$SrSnS$_4$, respectively. For ESI and crystallographic data in CIF or other electronic format see DOI: 10.1039/c9sc00028c

‡ Kui Wu and Yu Chu contributed equally.

transitions and several anionic groups, e.g., typical MS_4 (M = Ga, In, Ge, Sn) tetrahedra, act as critical "NLO active units" and provide the main contribution to the origin of the SHG response.[11] Recently, considering the structural and performance features of commercial IR NLO materials, a targeted element-cosubstitution strategy has been used to design new potential IR NLO materials by the replacement of cations or/and anionic groups with classical materials as templates.[12] For example, many diamond-like (DL) and chalcopyrite-like (CL) sulfides can be structurally designed from the prototype compound $AgGaS_2$.[13] With this in mind, the classical $AgGaS_2$ is chosen as a template, through substituting the Ag cation with alkali (Li, Na) and alkaline earth (Sr) metals and the GaS_4 anionic group with $M^{IV}S_4$ (M^{IV} = Ge, Sn) NLO active units to afford the successful discovery of four new noncentrosymmetric (NCS) sulfides in this work, A_2-$SrM^{IV}S_4$ (A = Li, Na; M^{IV} = Ge, Sn). The experimental results show that all of them exhibit excellent performances (E_g: 3.1–3.8 eV; d_{ij}: 0.5–0.8 × $AgGaS_2$) and achieve the optimal balance of wide E_g and good d_{ij}, which indicates that they satisfy the performance demands as outstanding IR NLO candidates and can further remove the low LDTs and TPA of commercial materials. Moreover, the above results also confirm the feasibility of the motif-optimization strategy for exploring new IR NLO materials.

Results and discussion

Single crystal X-ray analysis shows that $Li_2SrM^{IV}S_4$ crystallize in the $I\bar{4}2m$ space group whereas $Na_2SrM^{IV}S_4$ crystallize in the $R3c$ space group (Table S1†). Note that an interesting structural change is found in Na_2SrSnS_4 ($R3c$) and Na_2BaSnS_4 ($I\bar{4}2d$), but $Na_2SrM^{IV}S_4$ do not undergo the structural transformation with different M^{IV} (Ge to Sn) atoms in comparison with other reported analogues, such as Ag_2BaGeS_4 ($I\bar{4}2m$) vs. Ag_2BaSnS_4 ($I222$)[14] and Na_2BaGeS_4 ($R3c$) vs. Na_2BaSnS_4 ($I\bar{4}2d$)[12a] (Table S2†). Bond valences and the global instability index (GII) are also calculated and the results verify their structural reasonability (GII = 0.10–0.13) (Tables S3–S6†). Herein, we have chosen Li_2SrGeS_4 and Na_2SrSnS_4 as the representatives to depict their structural differences. As for Li_2SrGeS_4, its three-dimensional (3D) network structure is composed of 2D corner-sharing $(LiS_4)_n$ layers (Fig. 1a) and isolated GeS_4 ligands, where the Sr atoms are located in the tunnels (Fig. 1b); in other words, its structure can be also depicted as a 3D framework composed by the interconnection of edge-sharing SrS_8 dodecahedra with Li and Ge atoms located at the channels (Fig. 1c). More importantly, it appears that the interesting compression of the unit cell along the c-axis and Li_2SrGeS_4 can be considered as the "compressed CL material", which is also similar to the reported CL structures. According to the following equation of the structural distortion degree ($\Delta d = 2 - (c/a)$, a and c are the cell parameters),[15] the calculated results show that $Li_2SrM^{IV}S_4$ exhibit a large Δd (Ge: 0.815 vs. Sn: 0.811), thus leading to severe compression along the c axis because of the larger coordination number (8) of Sr atoms than only 4 in classical $AgGaS_2$ (Table S7†). Moreover, based on the similar structures of known Li-based compressed CL sulfides,[13b] the interlayer spacing between two adjacent $(LiS_4)_n$ layers (1 and 2) was also calculated and the

Fig. 1 (a) Corner-sharing $(LiS_4)_n$ layer; (b) whole crystal structure of Li_2SrGeS_4 (Sr−S bonds omitted for clarity); (c) 3D network structure composed of edge-sharing SrS_8 dodecahedra (Ge−S and Li−S bonds omitted for clarity); (d) comparison of the interlayer spacing between adjacent $(LiS_4)_n$ layers in Li-based materials.

interlayer spacing increases gradually from 2.5160 to 2.5497 Å with the increase of the cation radius of Sr^{2+} (1.40 Å) to Ba^{2+} (1.56 Å),[16] which indicates that a large cation radius corresponds to a wide interlayer spacing but is inversely proportional to the large Δd in compressed CL materials (Fig. 1d and Table S7†). This result may give us a feasible way to predict the interlayer spacing and Δd for new compressed CL materials.

$Na_2M^{II}SnS_4$ (M^{II} = Sr, Ba) undergo the interesting structural transformation (Sr, $R3c$ vs. Ba, $I\bar{4}2d$) with the different alkaline-earth metals (Fig. 2). Based on the previous analysis,[12a] the whole structure of Na_2SrSnS_4 can be depicted as the combination of numerous three-types of rings including the outermost 24-NaS_6-MR ring, inner fake ring (composed of six isolated SnS_4 tetrahedra) and innermost 6-(SrS_7)-MR circle (Fig. 2b). Interestingly, both of the similar isolated SnS_4 tetrahedron and NaS_6 octahedron exist in the structures of $Na_2M^{II}SnS_4$ although they

Fig. 2 (a) Crystal structure of Na_2BaSnS_4 along the c-axis: a 3D network composed of edge-sharing BaS_8 dodecahedra, and an edge and corner-sharing $(NaS_6)_n$ 3D network; (b) the whole structure of Na_2SrSnS_4: three-types of rings (outermost, inner, innermost), 24-NaS_6-MR, and 6-SrS_7-MR.

still have several obviously different structural features. The prominent structural difference is the connection modes of NaS_6 and BaS_8/SrS_7 polyhedra, for instance, the BaS_8 polyhedra connect with each other by sharing edges to form a 3D network in Na_2BaSnS_4 (Fig. 2a), whereas the SrS_7 ligands link together by sharing corners and edges to make up the tunnel structure in Na_2SrSnS_4; besides, note that the NaS_6 octahedra are connected together to form 24-MRs in Na_2SrSnS_4, which is obviously different from that (all Na atoms exist in the tunnels linking together to form a 3D framework structure) in Na_2BaSnS_4. Moreover, Na_2SrMS_4 show discriminated structures compared with those of Li_2SrMS_4 ($R3c$ $vs.$ $I\bar{4}2m$) because of the different coordination numbers for monovalent cations (Na: 6 $vs.$ Li: 4). We have also investigated the effect of distortion degrees ($\Delta d = (d(\text{longest}) - d(\text{shortest}))$ and $\Delta\theta = (\theta(\text{largest}) - \theta(\text{smallest}))$) of IS_4 tetrahedra (I =Ag, Cu, Na, Li) on the structural changes of the I_2–AE–M–S_4 system (Table S2†). The result shows that the distortion degrees (Δd and $\Delta\theta$) of IS_4 units exhibit significant changes while the series of compounds undergo the space group transformations. After analysis of their structural features, it is clear that their structural transformations have a close relationship with the sizes and coordination numbers of cations. The above results also verify that the variable structural dimensionality and symmetry can be attributed to the cationic size effect, and similar phenomena were discovered in many relative systems, such as $BaGa_4S_7$ ($Pmn2_1$)[11a] $vs.$ $PbGa_4S_7$ (Pc),[17a] Ba_2GeSe_4 ($P2_1/m$)[17b] $vs.$ Mg_2GeSe_4 ($Pnma$),[17c] $etc.$ More importantly, our previous work has also reported the rising structural symmetries (Cs, $P\bar{1}$; Rb, $P2_1/c$; α-K, $Aba2$; and Na, $P\bar{4}c2$) in the $A_2Hg_3Ge_2S_8$ (A = alkali metal) system with the element substitutions (Cs to Na).[18] Thus, a slight change of the cation size can lead to structural changes and future structure prediction should pay close attention to the effect of cation sizes on crystal structures.

Air-stable high quality single crystals of millimeter dimension for title compounds were successfully prepared by spontaneous crystallization in vacuum-sealed silica tubes (Fig. 4a and b). Their experimental XRD patterns are in agreement with the simulated ones derived from the crystal data, which further verify the purity of polycrystalline samples (Fig. 3). We have also compared the powder XRD patterns before and after melting for the title compounds. Comparison results show that all of them exhibit identical patterns before and after melting, which demonstrates that they are congruently melting compounds (Fig. S1†). Besides, as seen from Fig. S2,† there are no obvious absorption peaks in the range from 4000 to 500 cm^{-1}, which indicates that they have a wide IR transmission region (~20 μm). In addition, critical optical parameters including E_g, d_{ij} and LDTs of the title compounds were systematically measured. All of them exhibit a wider E_g than the benchmark $AgGaS_2$ (2.73 eV), such as Li_2SrGeS_4 (3.75 eV), Li_2SrSnS_4 (3.10 eV), Na_2SrGeS_4 (3.80 eV), and Na_2SrSnS_4 (3.12 eV), which is similar to those of other reported A_2BaMS_4 compounds (Fig. 4a and b). The above results also indicate that the cosubstitution of alkali or alkaline earth metals in the same main group has little influence on the material E_g, which can also be confirmed in relative systems including $AZn_4Ga_5S_{12}$ (A = K, Rb, Cs; ~3.65 eV)[19] and

Fig. 3 Powder XRD patterns of title compounds.

$A_3Ga_3PS_8Cl$ (A = K, Rb; 3.60 $vs.$ 3.65 eV).[10d] Besides, their shortwave absorption edges are lower than 400 nm and such a low absorption edge can remove the effect of harmful TPA at 1 μm for another classical $ZnGeP_2$; thus, recent mature laser sources ($e.g.$ 1.06 μm) may be utilized to achieve the frequency-conversion in the title compounds. Besides, based on density functional theory, their band structures have been calculated and the results indicate that their optical absorptions (2.20–2.84 eV) are mainly derived from the $M^{IV}S_4$ units for the title compounds (Fig. 5 and S3†). Moreover, a wide E_g is helpful to improve the LDT and further ensures the normal use without damage or breakdown under the high-power laser system for one of the materials. Recently, estimating the LDTs of new NLO compounds on powder samples has become a feasible method according to the previously reported research results.[20] Herein, powder LDTs of the title compounds were investigated under

Fig. 4 (a) Experimental bandgaps of Li_2SrGeS_4 and Li_2SrSnS_4 (inserted are the photographs of picked crystals); (b) experimental bandgaps of Na_2SrGeS_4 and Na_2SrSnS_4 (inserted are the photographs of picked crystals); (c) powder SHG responses of Li_2SrGeS_4 and Li_2SrSnS_4 $versus$ $AgGaS_2$; (d) powder SHG responses of Na_2SrGeS_4 and Na_2SrSnS_4 $versus$ $AgGaS_2$.

Fig. 5 Total and partial density of states (TDOS and PDOS) of title compounds: (a) Li_2SrGeS_4, (b) Li_2SrSnS_4, (c) Na_2SrGeS_4, and (d) Na_2SrSnS_4.

Fig. 6 Schematic diagram of designing new IR NLO materials by the motif-optimization with $AgGaS_2$ as the template and title compounds achieve the suitable balance of wide E_g and good d_{ij}.

the excitation of a 1.06 μm pulse laser with $AgGaS_2$ as the reference (Table S8†). The experimental result shows that the title compounds have higher LDTs than $AgGaS_2$, for example, Li_2SrGeS_4 and Na_2SrGeS_4 (10 × $AgGaS_2$), Li_2SrSnS_4 (5.0 × $AgGaS_2$), and Na_2SrSnS_4 (6.0 × $AgGaS_2$), which are comparable to those of other famous IR NLO crystals, such as $LiGaS_2$ (11 × $AgGaS_2$),[21] $LiInS_2$ (2.5 × $AgGaS_2$),[21] $HgGa_2S_4$ (3.0 × $AgGaS_2$),[22] $BaGa_4S_7$ (3.0 × $AgGaS_2$),[11a] and $BaGa_4Se_7$ (3.7 × $AgGaS_2$).[11b] Based on the high LDTs and low shortwave absorption edges, the title compounds have good potential to achieve the output of the high-power IR laser with mature lasers (Ti:Al_2O_3 or Nd:YAG) excitation sources in comparison with commercial IR NLO materials.

In view of the NCS structures of the title compounds, the common Kurtz and Perry method[23] was adopted to investigate their powder SHG responses with $AgGaS_2$ as the reference. As seen from Fig. 4, all of their SHG intensities show a gradually increasing trend with the increase of their particle sizes, respectively, indicating the type I phase-matching behavior that is of importance for the high-efficient laser output, which is also similar to those of relative Ba-based analogues. Note that they exhibit good SHG responses about 0.5 and 0.8 times that of $AgGaS_2$ ($d_{36} = 13.9$ pm V^{-1}) for the title thiogermanates (7.0 pm V^{-1}) and thiostannates (11.1 pm V^{-1}) at the maximum particle size (200–250 μm), respectively. Meanwhile, their SHG coefficients have also been calculated and the maximum values are 4.75 for Li_2SrGeS_4, 6.64 for Li_2SrSnS_4, 6.44 for Na_2SrGeS_4 and 7.07 pm V^{-1} for Na_2SrSnS_4, respectively, which are basically in agreement with the experimental results. Besides, their d_{ij} is comparable to those of famous Li-based IR NLO materials, such as $LiGaS_2$ ($d_{31} = 5.8$ pm V^{-1})[21] or $LiInS_2$ ($d_{31} = 7.25$ pm V^{-1}).[21] According to the above analysis, the title compounds exhibit excellent performances with a wide E_g (>3.0 eV) and good d_{ij} (>0.5 × $AgGaS_2$) that satisfy the proposed balance conditions and hence are outstanding IR NLO materials. Thus, all of them can be expected to act as promising NLO candidates in the IR region.

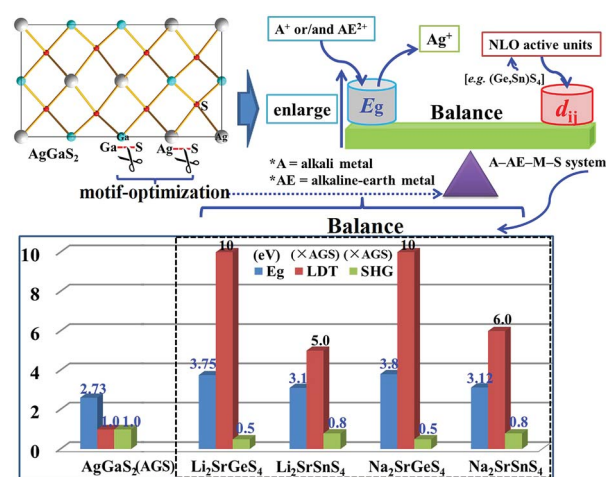Recently, an increasing number of IR NLO materials has been discovered by adopting the motif-optimization strategy with classical materials as templates based on the optimized atoms or/and anionic groups, such as DL or CL materials. Thus, this strategy has been proved to be an effective way to reorganize crystal structures and adjust physicochemical performances.[13] In this work, incorporation of electropositive alkali or/and alkaline earth metals (A^+/AE^{2+}) as cations and $M^{IV}S_4$ as "NLO active units" into the crystal structure of $AgGaS_2$ to replace the Ag^+ cation and GaS_4 units affords the successful discovery of a series of promising IR NLO materials and the optimization of alkali or alkaline earth metals in the same main group has little influence on the material E_g, which can be also confirmed in the successful discovery of a series of promising IR NLO materials and the research results also prove that the above design strategy is feasible (Fig. 6). Up to now, only 8 related IR NLO materials with excellent performances belonging to the A_2-$AEM^{IV}S_4$ (A = Li, Na; AE = Ba, Sr; M^{IV} = Ge, Sn) formula have been discovered (Table S9†). Thus, based on the above analysis, it can be concluded that the selection of cations or anionic groups should be extended to other A (K, Rb, Cs) and AE (Mg, Ca) elements or $M^{III}S_4$ ligands and the A–AE–M–S system should be identified as the preferred system for the future exploration of new IR NLO materials.

Conclusions

In summary, four potential IR NLO sulfides, $A_2SrM^{IV}S_4$, have been successfully discovered by the motif-optimization design strategy with classical $AgGaS_2$ as the template. $Li_2SrM^{IV}S_4$ exhibit compressed CL structures, whereas $Na_2SrM^{IV}S_4$ possess multiple rings and tunnel structures. Besides, analysis of the interlayer spacing (d) among CL materials shows that d has a close relationship with the cation radius and structural distortion degrees. Remarkably, all of them exhibit excellent performances, especially for the optimal balance of wide E_g and good d_{ij}. The discovery of the above materials also confirms that motif-optimization is an effective strategy to tune crystal

structures and performances and then further design promising IR NLO candidates. Furthermore, considering the characteristics of optimized cations or anionic groups, the A–AE–M–S system was identified as the preferred system for the future exploration of new IR NLO materials.

Conflicts of interest

There are no conflicts to declare.

Acknowledgements

Notes and references

1 (a) S. F. Li, X. M. Jiang, Y. H. Fan, B. W. Liu, H. Y. Zeng and G. C. Guo, Chem. Sci., 2018, 9, 5700; (b) T. T. Tran, H. W. Yu, J. M. Rondinelli, K. R. Poeppelmeier and P. S. Halasyamani, Chem. Mater., 2016, 28, 5238; (c) Y. Wang, B. B. Zhang, Z. H. Yang and S. L. Pan, Angew. Chem., Int. Ed., 2018, 57, 2150; (d) Z. G. Xia and K. R. Poeppelmeier, Acc. Chem. Res., 2017, 50, 1222; (e) P. Becker, Adv. Mater., 1998, 10, 979; (f) K. M. Ok, Acc. Chem. Res., 2016, 49, 2774; (g) Y. Pan, S. P. Guo, B. W. Liu, H. G. Xue and G. C. Guo, Coord. Chem. Rev., 2018, 374, 464; (h) X. F. Wang, Y. Wang, B. B. Zhang, F. F. Zhang, Z. H. Yang and S. L. Pan, Angew. Chem., Int. Ed., 2017, 56, 14119.

2 (a) R. L. Tang, C. L. Hu, F. F. Mao, J. H. Feng and J. G. Mao, Chem. Sci., 2019, 10, 837; (b) G. Q. Shi, Y. Wang, F. F. Zhang, B. B. Zhang, Z. H. Yang, X. L. Hou, S. L. Pan and K. R. Poeppelmeier, J. Am. Chem. Soc., 2017, 139, 10645; (c) F. Kong, S. P. Huang, Z. M. Sun, J. G. Mao and W. D. Cheng, J. Am. Chem. Soc., 2006, 128, 7750; (d) S. G. Zhao, P. F. Gong, S. Y. Luo, S. J. Liu, L. N. Li, M. A. Asghar, T. Khan, M. C. Hong, Z. S. Lin and J. H. Luo, J. Am. Chem. Soc., 2015, 137, 2207; (e) H. P. Wu, S. L. Pan, K. R. Poeppelmeier, H. Y. Li, D. Z. Jia, Z. H. Chen, X. Y. Fan and Y. Yang, J. Am. Chem. Soc., 2011, 133, 7786.

3 (a) X. S. Xing, R. J. Sa, P. X. Li, N. N. Zhang, Z. Y. Zhou, B. W. Liu, J. Liu, M. S. Wang and G. C. Guo, Chem. Sci., 2017, 8, 7751; (b) H. W. Yu, W. G. Zhang, J. Young, J. M. Rondinelli and P. S. Halasyamani, J. Am. Chem. Soc., 2016, 138, 88; (c) B. B. Zhang, G. P. Han, Y. Wang, X. L. Chen, Z. H. Yang and S. L. Pan, Chem. Mater., 2018, 30, 5397; (d) L. Xiong, J. Chen, J. Lu, C. Y. Pan and L. M. Wu, Chem. Mater., 2018, 30, 7823.

4 (a) G. H. Zou, Z. E. Lin, H. M. Zeng, H. Jo, S. J. Lim, T. S. You and K. M. Ok, Chem. Sci., 2018, 9, 8957; (b) G. H. Zou, N. Ye, L. Huang and X. S. Lin, J. Am. Chem. Soc., 2011, 133, 20001; (c) G. H. Zou, H. Jo, S. J. Lim, T. S. You and K. M. Ok, Angew. Chem., Int. Ed., 2018, 57, 8619; (d) J. Chen, L. Xiong, L. Chen and L. M. Wu, J. Am. Chem. Soc., 2018, 140, 14082.

5 (a) C. L. Hu and J. G. Mao, Coord. Chem. Rev., 2015, 288, 1; (b) M. Mutailipu, M. Zhang, H. P. Wu, Z. H. Yang, Y. H. Shen, J. L. Sun and S. L. Pan, Nat. Commun., 2018, 9, 3089.

6 (a) A. O. Okorogu, S. B. Mirov, W. Lee, D. I. Crouthamel, N. Jenkins, A. Y. Dergachev, K. L. Vodopyanov and V. V. Badikov, Opt. Commun., 1998, 155, 307; (b) G. D. Boyd, F. G. Storz, J. H. McFee and H. M. Kasper, IEEE J. Quantum Electron., 1972, 8, 900; (c) G. D. Boyd, E. Buehler and F. G. Storz, Appl. Phys. Lett., 1971, 18, 301.

7 (a) L. Kang, M. L. Zhou, J. Y. Yao, Z. S. Lin, Y. C. Wu and C. T. Chen, J. Am. Chem. Soc., 2015, 137, 13049; (b) F. Liang, L. Kang, Z. S. Lin and Y. C. Wu, Cryst. Growth Des., 2017, 17, 2254.

8 (a) I. Chung and M. G. Kanatzidis, Chem. Mater., 2014, 26, 849; (b) S. P. Guo, Y. Chi and G. C. Guo, Coord. Chem. Rev., 2017, 335, 44; (c) M. C. Chen, L. M. Wu, H. Lin, L. J. Zhou and L. Chen, J. Am. Chem. Soc., 2012, 134, 6058; (d) Z. Z. Luo, C. S. Lin, H. H. Cui, W. L. Zhang, H. Zhang, H. Chen, Z. Z. He and W. D. Cheng, Chem. Mater., 2015, 27, 914; (e) X. M. Jiang, S. P. Guo, H. Y. Zeng, M. J. Zhang and G. C. Guo, Struct. Bonding, 2012, 145, 1.

9 (a) T. K. Bera, J. I. Jang, J. B. Ketterson and M. G. Kanatzidis, J. Am. Chem. Soc., 2009, 131, 75; (b) J. C. Syrigos, D. J. Clark, F. O. Saouma, S. M. Clarke, L. Fang, J. I. Jang and M. G. Kanatzidis, Chem. Mater., 2015, 27, 255.

10 (a) B. W. Liu, H. Y. Zeng, X. M. Jiang, G. E. Wang, S. F. Li, L. Xu and G. C. Guo, Chem. Sci., 2016, 7, 6273; (b) Y. Y. Li, P. F. Liu and L. M. Wu, Chem. Mater., 2017, 29, 5259; (c) J. A. Brant, D. J. Clark, Y. S. Kim, J. I. Jang, J. H. Zhang and J. A. Aitken, Chem. Mater., 2014, 26, 3045; (d) J. A. Brant, D. J. Clark, Y. S. Kim, J. I. Jang, A. Weiland and J. A. Aitken, Inorg. Chem., 2015, 4, 2809; (e) K. Wu and S. L. Pan, Coord. Chem. Rev., 2018, 377, 191.

11 (a) X. S. Lin, G. Zhang and N. Ye, Cryst. Growth Des., 2009, 9, 1186; (b) J. Y. Yao, D. J. Mei, L. Bai, Z. S. Lin, W. L. Yin, P. Z. Fu and Y. C. Wu, Inorg. Chem., 2010, 49, 9212; (c) Y. Kim, I. S. Seo, S. W. Martin, J. Baek, P. S. Halasyamani, N. Arumugam and H. Steinfink, Chem. Mater., 2008, 20, 6048; (d) B. W. Liu, H. Y. Zeng, M. J. Zhang, Y. H. Fan, G. C. Guo, J. S. Huang and Z. C. Dong, Inorg. Chem., 2015, 54, 976.

12 (a) K. Wu, Z. H. Yang and S. L. Pan, Angew. Chem., Int. Ed., 2016, 55, 6713; (b) D. J. Mei, S. Y. Zhang, F. Liang, S. G. Zhao, J. Q. Jiang, J. B. Zhong, Z. S. Lin and Y. C. Wu, Inorg. Chem., 2017, 56, 13267.

13 (a) F. Liang, L. Kang, Z. S. Lin, Y. C. Wu and C. T. Chen, Coord. Chem. Rev., 2017, 333, 57; (b) K. Wu, B. B. Zhang, Z. H. Yang and S. L. Pan, J. Am. Chem. Soc., 2017, 139, 14885; (c) H. Chen, P. F. Liu, B. X. Li, H. Lin, L. M. Wu and X. T. Wu, Dalton Trans., 2018, 47, 429.

14 (a) C. L. Teske, *Z. Naturforsch.*, 1979, **34b**, 544; (b) L. Y. Nian, K. Wu, G. J. He, Z. H. Yang and S. L. Pan, *Inorg. Chem.*, 2018, **57**, 3434.

15 J. A. Aitken, P. Larson, S. D. Mahanti and M. G. Kanatzidis, *Chem. Mater.*, 2001, **13**, 4714.

16 F. C. Hawthorne, *Acta Crystallogr.*, 1994, **B50**, 481.

17 (a) X. S. Li, L. Kang, C. Li, Z. S. Lin, J. Y. Yao and Y. C. Wu, *J. Mater. Chem. C*, 2015, **3**, 3060; (b) A. Assoud, N. Soheilnia and H. Kleinke, *Z. Naturforsch.*, 2004, **59**, 975; (c) K. Wu, S. L. Pan and Z. H. Yang, *RSC Adv.*, 2015, **5**, 33646.

18 (a) J. H. Liao, G. M. Marking, K. F. Hsu, Y. Matsushita, M. D. Ewbank, R. Borwick, P. Cunningham, M. J. Rosker and M. G. Kanatzidis, *J. Am. Chem. Soc.*, 2003, **125**, 9484; (b) G. A. Marking, J. A. Hanko and M. G. Kanatzidis, *Chem. Mater.*, 1998, **10**, 1191; (c) K. Wu, Z. H. Yang and S. L. Pan, *Chem. Mater.*, 2016, **28**, 2795.

19 H. Lin, H. Chen, Y. J. Zheng, J. S. Yu, X. T. Wu and L. M. Wu, *Chem.–Eur. J.*, 2017, **23**, 10407.

20 (a) M. J. Zhang, X. M. Jiang, L. J. Zhou and G. C. Guo, *J. Mater. Chem. C*, 2013, **1**, 4754; (b) M. J. Zhang, B. X. Li, B. W. Liu, Y. H. Fan, X. G. Li, H. Y. Zeng and G. C. Guo, *Dalton Trans.*, 2013, **42**, 14223.

21 (a) L. Isaenko, A. Yelisseyev, S. Lobanov, A. Titov, V. Petrov, J. J. Zondy, P. Krinitsin, A. Merkulov, V. Vedenyapin and J. Smirnova, *Cryst. Res. Technol.*, 2003, **38**, 379; (b) L. Isaenko and I. Vasilyeva, *J. Cryst. Growth*, 2008, **310**, 1954.

22 V. Petrov, G. Marchev, A. Tyazhev, M. Beutler, V. Panyutin, M. Starikova, A. Esteban-Martin, V. Badikov, G. Shevyrdyaeva, D. Badikov, M. Reza, S. Sheina and A. Fintisova, *Opt. Eng.*, 2013, **52**, 117102.

23 S. K. Kurtz and T. T. Perry, *J. Appl. Phys.*, 1968, **39**, 3798.